

Accepted Manuscript

Detection and characterisation of Black Death burials by multi-proxy geophysical methods

Henry C. Dick, Jamie K. Pringle, Barney Sloane, Jay Carver, Austin Haffenden, Stephen Porter, Honorary Archivist, Daniel Roberts, Nigel J. Cassidy



PII: S0305-4403(15)00150-8

DOI: [10.1016/j.jas.2015.04.010](https://doi.org/10.1016/j.jas.2015.04.010)

Reference: YJASC 4413

To appear in: *Journal of Archaeological Science*

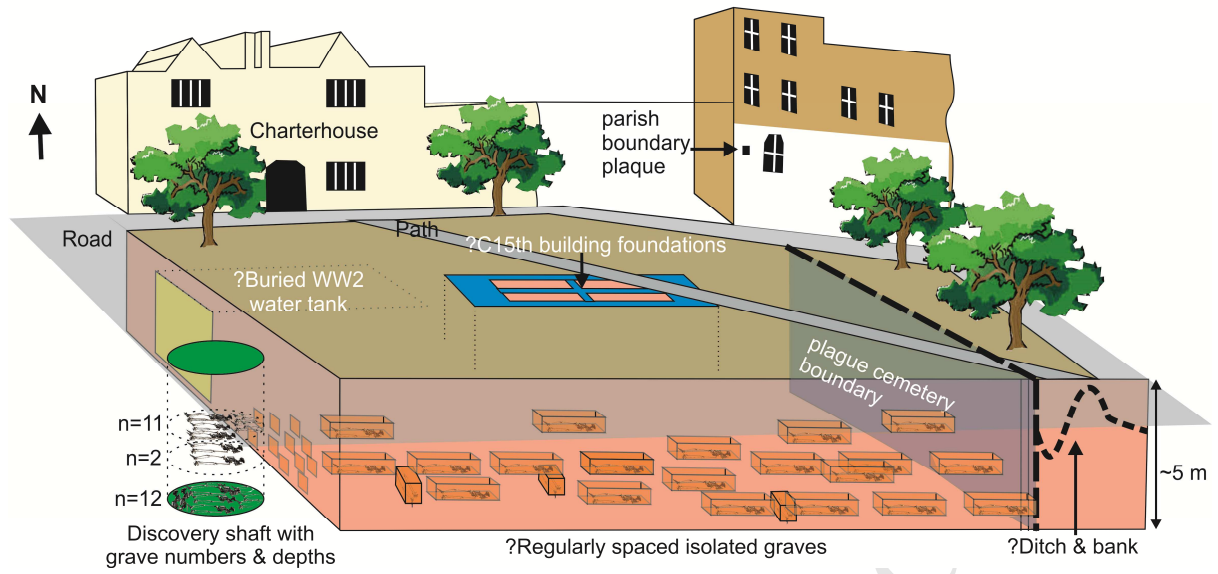
Received Date: 3 September 2014

Revised Date: 22 April 2015

Accepted Date: 23 April 2015

Please cite this article as: Dick, H.C., Pringle, J.K., Sloane, B., Carver, J., Haffenden, A., Porter, S., Roberts, D., Cassidy, N.J., Detection and characterisation of Black Death burials by multi-proxy geophysical methods, *Journal of Archaeological Science* (2015), doi: 10.1016/j.jas.2015.04.010.

This is a PDF file of an unedited manuscript that has been accepted for publication. As a service to our customers we are providing this early version of the manuscript. The manuscript will undergo copyediting, typesetting, and review of the resulting proof before it is published in its final form. Please note that during the production process errors may be discovered which could affect the content, and all legal disclaimers that apply to the journal pertain.



1 **Detection and characterisation of Black Death burials by multi-proxy geophysical methods**

2

3 Henry C. Dick^{a,b}, Jamie K. Pringle^{a*}, Barney Sloane^c, Jay Carver^d, Austin Haffenden^a, Stephen
4 Porter^e, Daniel Roberts^a, & Nigel J. Cassidy^a

5

6 ^aSchool of Physical Sciences & Geography, Keele University, Keele, ST4 6DA, UK. Email
7 address: h.c.dick@keele.ac.uk j.k.pringle@keele.ac.uk a.haffenden@keele.ac.uk;
8 dan.roberts35@gmail.com; n.j.cassidy@keele.ac.uk

9 ^bApplied Geophysics Group, Physics Dept., University of Port Harcourt, Nigeria

10 ^cEnglish Heritage, Swindon, UK. Email: barney.sloane@english-heritage.org.uk

11 ^dCrossRail Ltd, 25 Canada Square, Canary Wharf, London, E14 5LQ. UK. Email:
12 jaycarver@crossrail.co.uk

13 ^eHonorary Archivist, Sutton's Hospital in Charterhouse, London, UK. Email:
14 sc.porter@tiscali.co.uk

15

16 *Corresponding author: Keele University, School of Physical Sciences & Geography, William
17 Smith Building, Keele, ST4 6DA, UK. Tel: +44 (0)1782 733163. Email address:
18 j.k.pringle@keele.ac.uk.

19

20 **Keywords:** burials; plague; Black Death; London; geophysics

21 **Abstract**

22

23 The Crossrail underground network extension discovered 25 well preserved skeletons
24 shallowly buried in Central London in 2013. Subsequent carbon dating and aDNA analysis
25 confirmed the archaeological age and presence of the *Yersinia pestis* “Black Death” plague
26 epidemic strain. Here we present the non-invasive multi-proxy geophysical survey of the
27 adjacent Charterhouse Square, rapidly undertaken to detect any further burials and
28 characterise the site. Historical records suggested the area was a burial ground for Black
29 Death plague victims, before subsequent cemetery and urban land use. Following initial
30 trial surveys, surveys imaged ~200 isolated and similar-sized burials in the south-west of the
31 site. There were also two contrasting burial orientations present at various depths which
32 suggested a series of controlled phased burials. A well-defined eastern burial boundary,
33 taking the form of a ditch and bank, was also discovered. Geophysical surveys also
34 identified a subsequent complex site history with multiple-aged features. This study revises
35 knowledge of Black Death aged-burials and provides important implications for successful
36 geophysical burial detection with significant time- and space-limited site constraints.

37

38 1. Introduction

39

40 In 2013 Europe's biggest construction project, the Crossrail underground network extension,
41 discovered 25 well preserved skeletons, shallowly buried in close proximity to each other, in
42 Charterhouse Square in Central London. Historical records suggested that the site was an
43 emergency burial ground for Black Death victims during the 1348-1349 AD plague epidemic
44 (Porter, 2009; Sloane, 2011). A non-invasive archaeological geophysical survey of
45 Charterhouse Square with a limited time scale was commissioned because of active
46 construction deadlines.

47

48 There are generally accepted to be three plague pandemics in recorded human history,
49 Justinian's Plague (541-542 AD) that was mostly contained within Mediterranean countries,
50 the much wider European so-called Black Death plague (1345-1750 AD) and the 19th Century
51 Chinese plague epidemic which spread globally in 1894 AD (Haensch et al., 2010). The Black
52 Death was the first widespread outbreak of medieval plague in Europe, with recent
53 historical research estimating that it reduced London's population by 30% - 50 % between
54 1347-1351 AD (Sloane, 2011). Contemporary accounts detail the sheer numbers of dead
55 prevented Christian burials from being undertaken "*so great a multitude eventually died*
56 *that all the cemeteries of the aforesaid city were insufficient for the burial of the dead. For*
57 *this reason, many were compelled to bury their dead in places unseemly, not hallowed or*
58 *blessed; some, it was said, cast the corpses into the river*" (Sloane, 2011).

59

60 Recent scientific advancements in dating skeletal remains have allowed research into age of
61 mortality in London during this period (DeWitte, 2010; DeWitte & Hughes-Morey, 2012),
62 subsequent population health improvements (DeWitte, 2014) and confirmation of plague
63 strains to be rapidly identified, usually in the pulp of teeth (Kacki et al., 2004; Drancourt et
64 al., 2004; Bianucci et al., 2009; Haensch et al., 2010). Research has also cast doubt on the
65 traditionally-held premise that rats (*Rattus rattus/norvegicus*) formed the intermediate host
66 carrier in North European countries, with pneumonic (human to human via air droplets)
67 rather than bubonic plague now proposed to be the main dispersal method (Hufthammer &
68 Walloe, 2013).

69

70 Current search methods to detect both archaeological and modern human burials are highly
71 varied and have been reviewed (Hunter & Cox, 2005; Pringle et al., 2012a), with best
72 practice suggesting a phased approach, moving from large-scale remote sensing methods
73 (Kalacska, 2009), through to initial ground reconnaissance and control studies before full
74 searches are initiated (Harrison and Donnelly, 2009, Larsen et al., 2011). These full searches
75 can involve many and varied methods, depending upon the individual target(s) and site and
76 even seasonal parameters (see Pringle et al., 2012a; Jervis and Pringle, 2014) through to
77 physical excavation (e.g. see Hunter and Cox, 2005).

78

79 Near-surface geophysical surveys have been often applied in archaeological site
80 investigations, either to detect and/or characterise a site (e.g. see De Smedt et al., 2014) or
81 to decide where to start intrusive investigations. Archaeological geophysical searches for

82 unmarked burials are many and have had varied success, for example, locating
83 archaeological graves in Jordan (Frohlich and Lancaster, 1986) and Turkey (Arisoy et al.,
84 2007), Kings' Mounds in Sweden (Persson and Olofsson, 2004), Icelandic Viking/Medieval
85 graves (Damiata et al., 2013), North American Indian historic burial grounds (Bigman, 2012),
86 19th century cemeteries and graveyards in New Zealand (Nobes, 1999), the USA (Bevan,
87 1991; Ellwood et al., 1994; Doolittle & Bellantoni, 2010; Dalan et al., 2010; Honerkamp and
88 Crook, 2012; Bigman, 2014), Australia (Buck, 2003), the UK (Hansen et al., 2014), to 19th
89 century Irish Famine victims (Ruffell et al., 2009) and 20th century Svalbard Spanish Flu
90 victims (Davis et al., 2000). The advantages of archaeological surveys are that there is
91 usually little time constraint; however for forensic and time-limited geophysical surveys the
92 need to rapidly characterise a site and identify potential burial position(s) is paramount (e.g.
93 see Nobes, 2000; Pringle and Jervis, 2010; Novo et al., 2011).

94

95 Due to the limited survey time and site constraints, a multi-proxy geophysical rapid
96 assessment approach had to be used in this study. Study aims were : **firstly** to determine if
97 non-invasive geophysical methods could both detect and characterise the historic burial
98 ground; **secondly** to detect any further unmarked burials within the survey area and if there
99 were any particular concentrations and orientations; **thirdly** to determine the optimum
100 geophysical technique(s) for such an archaeological time-limited scenario and finally;
101 **fourthly** to compare results to other published studies.

102

103 2. Material and methods

104

105 2.1 Study site

106

107 The study site was at Charterhouse Square near St. Bartholomew's Hospital in Central
108 London, UK, situated ~1 km north of the Thames river and ~15 m above sea level (**Fig. 1**).
109 Charterhouse Square is a 4 acre urban grassed park containing isolated mature deciduous
110 trees, surrounded by roads and buildings with Charterhouse hospital itself to the north-west
111 (**Fig. 2**). Available British Geological Survey boreholes detail an organic-rich silty topsoil
112 succeeded by unconsolidated fluvial sands, gravels and alluvium from previous courses of
113 the River Thames that overlie Eocene London Clay and Cretaceous Chalk bedrock types at
114 ~30 m and ~50 m below ground level (bgl) respectively.

115

116 Historical records showed a 13 acre area north of the city walls (**Fig. 1**) was leased by Sir
117 Walter de Mauny in 1349 AD from St. Bartholomew's priory as a burial ground for The Black
118 Death plague victims (Hope, 1925). In 1371 AD de Mauny also sponsored a Carthusian
119 priory and enlarged the site by 4 Acres to the east, the boundary between these areas being
120 a parish boundary that still remains today (Porter, 2009), with a chapel built in 1481 AD and
121 the priory's meat kitchen (Temple, 2010). The priory was dissolved in 1538 AD with the
122 1348 AD chapel demolished in 1545 AD and the chapel erected in 1481 AD pulled down in
123 1615 AD; the meat kitchen was probably demolished c.1545 AD (Barber and Thomas, 2002).
124 The buildings of the former priory was rebuilt as a mansion, which was adapted in 1614 AD
125 as an almshouse and school, and after the priory's dissolution the periphery of its outer
126 precinct was built upon, enclosing the modern Charterhouse Square. The construction of

127 the London Metropolitan Railway and a new street built in the 1860s - 1870s AD encroached
128 upon the southern area of the site (Porter, 2009). In 1939 AD as part of World War Two air-
129 raid precautions, six underground emergency water tanks were installed in the square.
130 Lastly an exploratory excavation was undertaken in 1997-8 AD with an isolated skeleton
131 discovered in the north-east of the site (MoLAS, 1998).

132

133 **Figure 1:**

134 **Figure 2:**

135

136 2.2. Archaeological excavations

137

138 As part of the underground network extension, a 4.5 m diameter vertical shaft was dug on
139 the road to the south-west of the Square (**Fig. 2**). At 2.3 m bgl below compacted clay soil,
140 eight isolated earth-cut graves containing eleven relatively well preserved predominantly
141 human remains were encountered aligned northeast-southwest (**Fig. 3a**). These did not
142 show any signs of trauma although further disarticulated human remains were also
143 recovered from two of the grave fills. At 2.5 m bgl two isolated earth-cut graves containing
144 two relatively well preserved incomplete human remains were also encountered, again
145 aligned northeast-southwest. At 2.7 m bgl nine isolated earth-cut graves and one double-
146 grave containing eleven well preserved predominantly adult human remains were
147 encountered, nine aligned northeast-southwest and two aligned north-south (**Fig. 3b**). The
148 deepest burials had two graves with multiple burials, one with remains on top of the first
149 and the other having them side by side (**Fig. 3b**). Recovered pottery shards from the 2.3m
150 bgl burials estimated a burial date of 1270-1350 AD.

151

152 Subsequent radio-carbon dating of the 2.5 m and 2.7 m bgl burials gave date ranges of 1275
153 AD -1405 AD ± 20 BP, with the 2.3 m bgl burials having a date range of 1430 AD – 1485 AD
154 ± 21 BP (see MoLAS, 2013). Rapid aDNA analysis (see Kacki et al., 2004) of the recovered
155 human remains confirmed the presence of the *Yersinia pestis* Black Death plague epidemic
156 strain in all three burial phases (**Fig. 3** and MoLAS, 2013).

157

158 **Figure 3:**

159

160 *2.3 Near-Surface geophysical investigations*

161

162 After initial trial surveys showed detectable anomalies following best practice (see Milsom
163 and Eriksen, 2011), a two day time-limited survey was then undertaken. 2D profile positions
164 (**Fig. 2a**) were all surveyed using a Leica™ 1200 total station theodolite and reflector prism
165 with an 0.005 m average position accuracy before being integrated with the digital sitemap
166 in ArcGIS™ ArcMap v.10 software.

167

168 A bulk ground conductivity survey was undertaken over the whole square using a Geonics™
169 EM-31-Mark2 conductivity meter (**Suppl. Mat.**), not to identify individual grave positions but
170 in order to rapidly characterise the site and to determine the spatial limits of the burial area.
171 This instrument images bulk changes in the near-surface, typically down to ~10m bgl in ideal
172 conditions (see Milsom and Eriksen, 2011). It was expected that there should be a
173 measureable EM contrast across the burial area margins, any relict building infrastructure to

174 be clearly imaged as isolated high/low linear anomalies and the highly conductive water
175 tanks to be found if remaining. The instrument was zeroed at the northeast side of the
176 square which was determined to be relatively geophysically homogeneous from the trial
177 surveys. Due to potential cultural interference from above-ground conductive objects, the
178 dataset was collected with the meter in vertical orientation (VMD) mode which did reduce
179 its sensitivity to very near-surface objects (see Milsom and Eriksen, 2011). Both inphase and
180 quadrature data types were collected on 2 m spaced survey lines in a one-way, west-east
181 orientation across the square at ~0.5 m spatial position increments. A Garmin™ GPS also
182 logged sample positions and was used by Trackmaker31™ v.1.21 to check positional
183 locations. Standard post-survey data processing was undertaken in Geoscan™ Geoplot
184 v3.00 software, including data de-spiking to remove isolated anomalous data points and de-
185 trending to remove long wavelength site trends from the data, before the dataset was
186 imported into ARCGIS ArcMAP™ v.10 software and a digital, colour contoured surface was
187 generated using ordinary kriging through the Geostatistical Analyst extension.

188

189 An electrical resistivity survey was only collected over the south-west area of the site due to
190 time constraints as other studies (see e.g. Hansen et al., 2014; Ellwood et al., 1994) have
191 imaged relative low/high isolated resistivity anomalies associated with historic burials,
192 compared to background values. Whilst 0.5 m probe spacing configurations are commonly
193 used for such investigations (see e.g. Hansen et al., 2014; Pringle and Jervis, 2010), a 1 m
194 probe separation was used here to penetrate to the ~3 m depths of the discovered graves
195 (**Fig. 3**). Remote probes were set at least 10 m from sample positions following best
196 practice guidelines (see Milsom and Eriksen, 2011). Geoscan™ RM15-D bulk ground

197 electrical resistivity equipment (**Suppl. Mat.**), with a stated measurement accuracy of 0.1 Ω ,
198 was used to collect 1 m x 0.1 m spaced data over a limited area of 8 m x 38 m, located
199 adjacent to the discovered burials (L1-8 in **Fig.2** for location). After data download, standard
200 post-survey data processing were undertaken in Geoscan™ Geoplot v.3.00 software,
201 including; (i) conversion of measured resistance (Ω) values to apparent resistivity ($\Omega.m$) to
202 account for probe configuration; (ii) data de-spiking to remove isolated anomalous data
203 points and; (iii) dataset de-trending to remove long wavelength site trends from the data
204 (see Milsom and Eriksen, 2011). The dataset was then imported into ARCGIS ArcMAP™ v.10
205 software and a digital, colour contoured surface was generated using ordinary kriging
206 through the Geostatistical Analyst extension.

207

208 A Ground Penetrating Radar (GPR) dataset was also collected over the south-west area of
209 the site, as other authors have found this method effective to detect unmarked
210 archaeological burials as discussed in the introduction. Due to time constraints, widely-
211 spaced and orientated 2D profiles were also collected in the rest of the square to detect if
212 further graves were present, and to determine the spatial burial area extent and its margins
213 (**Fig. 2** for location). After the trial surveys determined the optimum radar frequency, GPR
214 PulseEKKO™ 1000 equipment was utilised with 225 MHz frequency antennae and a 32 v
215 transmitter antennae (**Suppl. Mat.**) to collect the data with 0.1 m trace spacings , 90 ns time
216 window and constant 32 repeat stacks. A grid of 1-m spaced 2D profiles were acquired
217 adjacent to the discovered archaeological graves (L1-21), three (L22-24) acquired on the
218 road to the north of the square, two (L25,29) orientated at right angles to the parish
219 boundary, one (L26) outside the parish boundary and a final profile (L28) mid-way across

220 the square. Standard data processing steps were undertaken in REFLEX-Win™ v.3.0
221 processing software, these included; (1) subtracting the mean from traces; (ii) picking first
222 arrivals and then (iii) applying static correction and moved trace start times to 10 ns; (iv)
223 time-cut to remove blank data and; (v) manual gain 1D filter to boost relative deeper radar
224 trace amplitudes whilst retaining shallow ones.

225

226 Two 2D Electrical Resistivity Imaging (ERI) profiles, orientated at right angles to the known
227 parish boundary, were also collected by a CAMPUS™ TIGRE system (**Suppl. Mat.**) to
228 determine if this marked the burial margin (**Fig.2** for location). As with the conductivity
229 data, it would be expected that there would be a sharp contrast in resistive properties
230 across this margin. Both profiles used 32 steel electrodes inserted into the ground along
231 each profile, with ERI1 and ERI2 using 1 m and 0.5 m probe spacing respectively due to site
232 constraints. ImagerPro™ 2000 data acquisition software used a Wenner configuration and
233 10 'n' levels that should penetrate to ~5 m bgl as shown by other researchers (see e.g.
234 Brown, 2006; Pringle et al., 2012b). Raw ERI datasets were then individually processed with
235 anomalous data points removed and inverted utilizing least-square inversions in Geotomo™
236 Res2Dinv v.355 software following standard methods (see Milsom and Eriksen, 2011). Half
237 cell spacing was also utilized during the inversion process to remove potential edge effects
238 and reduce any probe contact resistance variations. Finalised models of true resistivity
239 sections were created with a relatively small RMS mis-fit of 2.5 % (ERI1) and 4.1 % (ER2)
240 between the respective calculated models and acquired datasets (see Milsom and Eriksen,
241 2011).

242

243 3. Results

244 The processed bulk ground EM conductivity dataset, acquired in order to characterise the
245 site and determine the spatial limits of the burial area, showed a relatively highly conductive
246 15 m² rectangular area in the north-west of the square, compared to background values,
247 which will most probably be the location of the WW2 water tank (**Fig. 4**). There was also a
248 relatively high conductive area in the south, but this was probably due to the presence of
249 the above-ground metal fence that bordered the urban square. There was a relative low
250 conductive ~25 m² area in the north-east of the square whose origin could not be
251 determined (**Fig. 4**). In contrast, there was also a ~20 m² square anomaly with variable
252 relative high/low conductive values in the central area (**Fig. 4**); this was of similar size to a
253 meat kitchen documented to be onsite. Interestingly there was no measureable difference
254 in EM properties across the parish boundary as was expected (**Fig. 4**).

255

256 **Figure 4:**

257

258 The processed electrical resistivity survey of the south-west area of the square, adjacent to
259 the discovery shaft, showed a trend from very high resistivity values in the south to very low
260 resistivity values to the north (**Fig. 5**). The north area therefore agrees with the high
261 conductivity values in the EM dataset. However relative isolated anomalies compared to
262 background values, which may be expected from individual graves containing human
263 remains (see Frohlich & Lancaster, 1986; Hansen et al. 2014), were disappointingly not
264 observed in this dataset. This may be due to this survey not penetrating to their likely 2+ m
265 depths below ground level.

266 **Figure 5:**

267

268 The processed 2D GPR profiles in the western of the square (L1-21 – see **Fig. 2**) consistently
269 imaged isolated, evenly-spaced and similar-sized $\frac{1}{2}$ hyperbolic reflection events produced
270 from buried objects in the southern half of all profiles (**Fig. 6**). These objects were between
271 ~ 1.5 m to ~ 3 m bgl that were similar to the discovered historic graves (**Fig. 3**) and have been
272 observed in other mass burials (e.g. Ruffell et al., 2009). Smaller and shallower $\frac{1}{2}$ hyperbolic
273 reflection events were due to tree roots from mature deciduous trees onsite. Consistent,
274 very strong horizontal reflections for ~ 10 m – 12 m were also present at the northern end
275 (**Fig. 6**), with both a top at ~ 0.5 m bgl and bottom ~ 2 m bgl reflector observed (*cf.* **Fig. 6**).
276 This significant-sized object was correlated to the high conductivity/low resistivity anomaly
277 present in both the EM and electrical resistivity datasets respectively and was the water
278 tank. Due to time constraints the profiles were too widely-spaced for meaningful horizontal
279 time slices to be generated.

280

281 The other 2D profile (L28) across the park (**Fig. 2** for location) showed multiple isolated $\frac{1}{2}$
282 hyperbolic reflection events in the southern side, with none present in the north, although
283 there was no strong horizontal reflector present (**Fig. 6**). Three 2D profiles (L22-24) on the
284 north to the north of the square (**Fig. 2** for location) did not image any objects, except
285 beside observed surface manhole covers. The 2D profile (L26) that was located east of the
286 parish boundary did not show any characteristic isolated $\frac{1}{2}$ hyperbolic reflection events (**Fig.**
287 **6**).

288

289 **Figure 6:**

290

291 Both 2D ERI inverted models showed a clear contrast in resistivity properties across the
292 parish boundary, with relative higher resistivity values to the east of boundary and lower
293 values to the west, in contrast to the EM data (cf. Figs. 4 and 7). However, the GPR showed
294 much better resolution at this location, resolving a potential ditch and bank geometry at the
295 margin (**Fig. 7**). There were significant heterogeneities present in both profiles, as would be
296 expected in such urban environments, variable moisture content may also be a factor here
297 as others have found (Pringle et al., 2012b), especially in parklands (Jones et al., 2009).

298

299 **Figure 7:**

300

301 **4. Discussion**

302

303 The first aim of this study was “to determine if non-invasive geophysical methods could both
304 detect and characterise the historic burial ground”. The geophysical surveys have identified
305 the key characteristics of the site. These confirmed that the eastern boundary was the
306 marked parish boundary, a square anomaly in the centre may be buried foundations of the
307 priory’s meat kitchen, shown on mid-fifteenth century plans to have been a two-story
308 building, or, perhaps less likely, a demolished chapel. WW2 buried water tanks remain in
309 the north-west area and lastly, but most importantly, a concentration of ~200 isolated
310 buried objects were present in the south-west of the square. These 200 objects were most
311 probably further, and as yet undiscovered, isolated graves of Black Death plague victims
312 although this will need to be excavated for confirmation. The eastern boundary also had a
313 central ditch and eastern raised bank identified by GPR that that matched historical
314 accounts (Porter, 2009). **Figure 8** and **Table 1** summarise the study findings. These targets
315 were still geophysically detectable in a difficult urban survey environment, the burials after
316 660+ years, showing that archaeological geophysical surveys can both detect and
317 characterise historic burial sites. Note that any further archaeological targets in the
318 Square’s boundaries may not have been geophysically resolved due to local cultural noise.

319

320 **Figure 8:**

321

322 **Table 1.**

323 The second aim of this study was “to detect any further unmarked burials and if there were
324 any particular burial concentrations and orientations”. The SW of the square showed
325 multiple, evenly-spaced and shallow buried objects which were most likely to be historic
326 graves (**Fig. 8**). Simple identification of anomalies in GPR 2D profiles gave a conservative
327 estimate of ~200 individual graves; note that there will, most probably, be more due to co-
328 mingled remains as both this study (**Fig. 3**) and others, for example, the Kacki et al. (2011)
329 study of contemporary remains in French cemeteries, have evidenced. Historical records
330 suggest that there may be several thousand individuals buried in this area (see Sloane,
331 2011), but it was unknown what burial style they may be, and if they had been removed
332 subsequently. The mostly isolated nature of burials was surprising; it was documented that
333 burials during the height of the Black Death plague epidemic were buried in mass pits
334 (Sloane, 2011) and thus this study has revised the knowledge of burials to more of an
335 emergency cemetery style. The discovered burials also had three clearly different burial
336 phases, with clay-rich soil being deposited between each, perhaps in an attempt to prevent
337 the spread of the disease (**Fig. 8**). Some geophysical anomaly orientations were similar to
338 the discovered graves, approximately northeast-southwest, but there were other
339 orientations, north-south orientated burials for example. There do not seem to be remains
340 in the north of the Square and indeed outside the eastern parish boundary.

341

342 The third aim of this study was “to determine the optimum geophysical technique(s) for such
343 an archaeological time-limited scenario”. To successfully detect and characterise historic
344 burials a multi- phased approach using different geophysical techniques should be
345 undertaken following best practise (see Harrison & Donnelly, 2009; Larsen et al., 2011;

346 Pringle et al., 2012a). In this case, after the desk study of historical records and remote
347 sensing data had identified the burial site, during initial site reconnaissance, as well as soil
348 and bedrock type being determined, trial surveys using available non-invasive geophysical
349 equipment were undertaken. Electro-magnetic, electrical resistivity and GPR methods were
350 all trialled to determine if targets were geophysically detectable, i.e. measureable from
351 background values. EM surveys then rapidly surveyed the site, with bulk ground change
352 areas being identified. These areas were then re-surveyed by higher resolution geophysical
353 methods, particular GPR, and this phased approach is recommended for other studies. Trial
354 surveys also determined optimal geophysical equipment configurations. For example, GPR
355 225 MHz frequency antennae were judged optimal, mid-range frequency have also been
356 shown by other studies to detect buried archaeological objects buried at least 1 m depth bgl
357 (see Davis et al., 2000; Ruffell et al. 2009; Ruffell & Kulesa 2009; Hansen et al., 2014) which
358 gave confidence in the survey data collected. The electrical resistivity survey equipment
359 configuration was also used with 1 m electrode spacing on mobile probes, a less-used
360 spacing as 0.5 m is conventional (see Pringle et al., 2012b; Hansen et al., 2014) but one
361 deemed to be able penetrate to the desired depth bgl. Whilst the WW2 underground tanks
362 were identified, individual remains were not using this method; this was most probably due
363 to the heterogeneous nature of the site. ERI 2D profiles were judged very useful in this
364 study to characterise the burial boundaries, but the GPR 2D profiles on the same survey lines
365 had better resolution and allowed the nature of the boundary to also be determined.
366 Combining different geophysical techniques to gain extra information has also been
367 recommended by other authors (e.g. see Milsom & Eriksen, 2011; Pringle et al., 2012b).
368

369 The fourth and final aim of this study was “*to compare results to other published studies*”. In
370 the literature GPR has been commonly used to detect archaeological graves, for example
371 ancient graves in Jordan (Frohlich & Lancaster, 1986) and Viking/Medieval graves in Iceland
372 (Damiata et al., 2013), and unmarked graveyard and cemetery burials in New Zealand
373 (Nobes, 2000), Australia (Buck, 2003), the US (Doolittle & Bellantoni, 2013), Ireland (Rufell et
374 al., 2009) and the UK (Hansen et al., 2014), and marked burials in Germany (Fiedler et al.,
375 2009b). These studies have all used mid-range GPR antennae which this study has also
376 utilised after trial surveys. There are fewer published studies using electrical resistivity to
377 locate individual remains and indeed characterise mass burial sites, Witten et al. (2001)
378 used electrical resistivity to locate a 1920s race riot burial site in the US and Brown (2006)
379 used ERI 2D profiles to locate 1990s burials in Bosnia. For bulk ground conductivity De
380 Smedt et al. (2014) documented an EM survey to characterise the Stonehenge
381 archaeological site, but there is only Bigman’s (2012) study to locate unmarked graves in
382 North American Indian burial grounds and Nobes (2000) New Zealand clandestine grave
383 search. However all of these were in rural environments which was not the case here, albeit
384 De Smedt et al. (2014) documented advanced processing was needed to remove the effect
385 of near-surface metallic clutter from the data. From the data in this study it is suggested to
386 use EM techniques to characterise the site before using ERI 2D profiles to characterise site
387 margins, followed by mid-frequency radar surveys to characterise their content. It was
388 impressive that near-surface geophysical surveys have been so effective in such a busy
389 urban environment.

390

391 **4. Conclusions**

392

393 Following the discovery of historic skeletal remains and subsequent radiocarbon dating and
394 aDNA analysis confirmed individuals were victims of the *Yersinia pestis* Black Death plague
395 epidemic in the 14th and 15th Centuries, a multi-technique near-surface geophysical survey
396 was undertaken in Charterhouse Square in central London. An EM, ERI and GPR survey
397 rapidly characterised the site, finding the eastern boundary of a burial ground with
398 suspected ditch and bank that matched historical records. There were concentrations of
399 ~200 surprisingly isolated burials in the south-west of the site, with two different burial
400 orientations and three different burial depths below ground level. These suggest different
401 phases of burial over different time periods that was confirmed by radiocarbon dating. The
402 square formed part of an emergency cemetery at this time, rather than mass burial
403 pits/trenches that was documented in historical records. Geophysical investigations also
404 characterised the site with subsequent demolished building foundations and WW2 water
405 tanks remaining on site. This study revised existing knowledge of Black Death burials and
406 shows the potential of near-surface geophysical techniques to both detect and characterise
407 historic mass burials in busy and restrictive urban environments.

408

409 **5. Acknowledgements**

410

411 This study was financially supported by TrueNorthTV Productions. Sarah Aldridge from
412 University College London and Matteo Giubertoni from Polimi University are acknowledged
413 for field assistance. A 2003 SRIF3 grant supported the purchase of geophysical and survey
414 equipment at Keele University.

415

ACCEPTED MANUSCRIPT

416 **6. References**

417

418 M.O. Arisoy, O. Kocak, A. Buyuksarac, F. Bilim, Images of buried graves in Bayat, Afon
419 (Turkey) from high-resolution magnetic data and their comparisons with preliminary
420 excavations. *J. Arch. Sci.* 34 (2007) 1473-1484. DOI:10.1016/j.jas.2006.11.005

421

422 B. Barber, C. Thomas, *The London Charterhouse*, Museum of London Archaeology Service,
423 10, 2002, pp. 73-74.

424

425 B.W. Bevan, The search for graves, *Geophys.* 56 (1991) 1310–1319. DOI:10.1190/1.1443152

426

427 R. Bianucci, L. Rahalison, A. Peluso, E.R. Massa, E. Ferroglio, M. Signoli, J-Y. Langlois, V.
428 Gallien, Plague immunodetection in remains of religious exhumed from burial sites in
429 central France, *J. Arch. Sci.* 36 (2009) 616-621. DOI:10.1016/j.jas.2008.10.007

430

431 D.P. Bigman, Mapping social relationships: geophysical survey of a 19th Century American
432 slave cemetery, *Arch. Anthro. Sci.* 6 (2014) 17-30. DOI:10.1007/s12520-013-0119-6

433

- 434 D.P. Bigman, The use of electromagnetic induction in locating graves and mapping
435 cemeteries: an example from Native North America, *Arch. Prosp.* 19 (2012) 31-39.
436 DOI:10.1002/arp.1416
- 437
- 438 A.G. Brown, The use of forensic botany and geology in war crimes investigations in NE
439 Bosnia. *For. Sci. Int.* 163 (2006) 204-210. DOI:10.1016/j.forsciint.2006.05.025
- 440
- 441 S.C. Buck, Searching for graves using geophysical technology: field tests with ground
442 penetrating radar, magnetometry and electrical resistivity, *J. Forensic Sci.* 48 (2003) 5–11.
443 DOI:10.1520/JFS2002165
- 444
- 445 R.A. Dalan, S.L. De Vore, R.B. Clay, Geophysical identification of unmarked historic graves,
446 *Geoarch.* 25 (2010) 572-601. DOI: 10.1002/gea.20325
- 447
- 448 B.N. Damiata, J.M. Stien berg, D.J. Bolender, Imaging skeletal remains with ground-
449 penetrating radar: comparative results over two graves from Viking Age and Medieval
450 churchyards on the Stóra-Seyla farm, northern Iceland. *J. Arch. Sci.* 40 (2013) 268-278.
451 DOI:10.1016/j.jas.2012.06.031
- 452

453 J.L. Davis, J.A. Heginbottom, A.P. Annan, R.S. Daniels, B.P. Berdal, et al., Ground penetrating
454 radar surveys to locate 1918 Spanish flu victims in permafrost, *J. Forensic Sci.* 45 (2000) 68–
455 76. DOI:10.1520/JFS14642J

456

457 S.N. DeWitte, Mortality risk and survival in the aftermath of the Medieval Black Death.
458 *PLoSone* 9 (2014) e96513. DOI:10.1371/journal.pone.0096513

459

460 S.N. DeWitte, G. Hughes-Morey, Stature and frailty during the Black Death: the effect of
461 stature on risks of epidemic mortality in London, A.D.1348-1350. *J Arch. Sci.* 39 (2012) 1412-
462 1419. DOI:10.1016/j.jas.2012.01.019

463

464 S.N. DeWitte, Age patterns of mortality during the Black Death in London, A.D. 1349-1350. *J*
465 *Arch. Sci.* 37 (2010) 3394-3400. DOI:10.1016/j.jas.2010.08.006

466

467 J.A. Doolittle, N.F. Bellantoni, The search for graves with ground-penetrating radar in
468 Connecticut, *J. Arch. Sci.* 37 (2010) 941 – 949. DOI:10.1016/j.jas.2009.11.027

469

470 M. Drancourt, V. Roux, L.V. Dang, L. Tran-Hung, D. Castex, V. Chenal-Francisque, H. Ogata, P-
471 E Fournier, E. Crubezy, D. Raoult, Genotyping, Orientalis-like *Yersinia pestis*, and Plague
472 Pandemics. *Emerg. Inf. Diseases*, 10 (2004) 1585-1592. DOI:10.3201/eid1009.030933

473

474 B.B. Ellwood, D.W. Owsley, S.H. Ellwood, P.A. Mercado-Allinger, P.A, Search for the grave of
475 the hanged Texas gunfighter, William Preston Longley, *Hist. Arch.* 28 (1994) 94–112.

476 <http://www.jstor.org/stable/25616320>

477

478 S. Fiedler, B. Illich, J. Berger, M. Graw, The effectiveness of ground-penetrating radar surveys
479 in the location of unmarked burial sites in modern cemeteries, *J. App. Geophys.* 68 (2009b)

480 380–385. DOI:10.1016/j.jappgeo.2009.03.003

481

482 B. Frohlich, W.J. Lancaster, Electromagnetic surveying in current Middle Eastern archaeology
483 – application and evaluation, *Geophys.* 51 (1986) 1414-1425. DOI:10.1190/1.1442190

484

485 S. Haensch, R. Bianucci, M. Sgnoli, M. Rajerison, M. Schultz, S. Kacki, M. Vermunt, D.A.

486 Weston, D. Hurst, M. Achtman, E. Carniel, B. Bramanti, Distinct clones of *Yersinia pestis*

487 caused the Black Death, *PLoS pathogens* 6 (2010) e1001134

488 DOI:10.1371/journal.ppat.1001134

489

490 J.D. Hansen, J.K. Pringle, J. Goodwin, GPR and bulk ground resistivity surveys in graveyards:
491 locating unmarked burials in contrasting soil types, *For. Sci. Int.* 237, (2014) e14-e29.

492 DOI:10.1016/j.forsciint.2014.01.009

493

494 M. Harrison, L.J. Donnelly, Locating concealed homicide victims: developing the role of
495 geoforensics, in: K. Ritz, L. Dawson, D. Miller, (Eds.), *Crim. and Env. Soil For.*, Springer, 2009,
496 pp. 197–219. ISBN 978-1-4020-9204-6

497

498 N. Honerkamp, R. Crook, Archaeology in a Geechee graveyard, *SE Arch.* (2012) 103-114.

499

500 W. Hope, St. John, *The History of the London Charterhouse*, 1925, pp.7-8.

501

502 A.K. Hufthammer, L. Walløe, Rats cannot have been intermediate hosts for *Yersinia pestis*
503 during medieval plague epidemics in Northern Europe. *J Arch. Sci.* 40 (2013) 1752-1759.
504 DOI:10.1016/j.jas.2012.12.007

505

506 J. Hunter, M. Cox, M. *Forensic archaeology: advances in theory and practice*. Routledge
507 (2005).

508

509 J.R. Jervis, J.K. Pringle, A study of the affect of seasonal climatic factors on the electrical
510 resistivity response of three experimental graves, *J App. Geophys.* 108 (2014) 53-60. DOI:
511 10.1016/j.jappgeo.2014.06.008

512

- 513 G.M. Jones, N.J. Cassidy, P.A. Thomas, S. Plante, J.K. Pringle, Imaging and monitoring tree-
514 induced subsidence using electrical resistivity tomography, *Near. Surf. Geophys.* 7 (2009)
515 191-206. DOI:10.3997/1873-0604.2009017
- 516
- 517 A. Juerges, J.K. Pringle, J.R. Jervis P. Masters, Comparisons of magnetic and electrical
518 resistivity surveys over simulated clandestine graves in contrasting burial environments,
519 *Near Surf. Geophys.* 8 (2010) 529–539. DOI:10.3997/1873-0604.2010041
- 520
- 521 S. Kacki, L. Rahalison, M. Rajerison, E. Ferroglio, R. Bianucci, Black Death in the rural
522 cemetery of Saint-Paurent-de-la-Cabrerisse Aude-Languedoc, southern France, 14th century:
523 immunological evidence. *J. Arch. Sci.* 38 (2011) 581-587. DOI:10.1016/j.jas.2010.10.012
- 524
- 525 M. Kalacska, L.S. Bell, G.A. Sanchez-Azofeifa, T. Caelli, The application of remote sensing for
526 detecting mass graves: an experimental animal case study from Costa Rica. *J. For. Sci.* 54
527 (2009) 159-166. DOI:10.1111/j.1556-4029.2008.00938.x
- 528
- 529 D.O. Larson, A.A. Vass, M. Wise, Advanced scientific methods and procedures in the forensic
530 investigation of clandestine graves. *J. Contemp. Crim. Just.* 27 (2011) 149–182.
531 DOI:10.1177/1043986211405885
- 532

- 533 J. Milsom, A. Eriksen. *Field Geophysics*. 4th ed. Wiley, 2011.
- 534
- 535 Museum of London Archaeology Service (MoLAS), *A Black Death cemetery at Charterhouse*
536 *Square, London EC1*, 2013, pp. 364-370.
- 537
- 538 Museum of London Archaeology Service (MoLAS), *Charterhouse Square, An Archaeological*
539 *Evaluation*, 1998, pp. 16.
- 540
- 541 D.C. Nobes, The search for “Yvonne”: a case example of the delineation of a grave using
542 near-surface geophysical methods, *J. For. Sci.* 45 (2000) 715–721. DOI:10.1520/JFS14756J
- 543
- 544 D.C. Nobes, Geophysical surveys of burial sites: a case study of the Oaro Urupa site,
545 *Geophys.* 64 (1999) 357–367. DOI:10.1190/1.1444540
- 546
- 547 A. Novo, H. Lorenzo, F. Ria, M. Solla, 3D GPR in forensics: finding a clandestine grave in a
548 mountainous environment, *For. Sci. Int.* 204 (2011) 134-138.
549 DOI:10.1016/j.forsciint.2010.05.019
- 550

551 K. Persson, B. Olofsson, Inside a mound: applied geophysics in archaeological prospecting at
552 the Kings' Mounds, Gamla Uppsala, Sweden, *J. Arch. Sci.* 31 (2004) 551-562.

553 DOI:10.1016/j.jas.2003.10.003

554

555 S. Porter, *The London Charterhouse*, Amberley Pubs., 2009, pp. 107. ISBN: 978-1848680906

556

557 J.K. Pringle, A. Ruffell, J.R. Jervis, J.D. Donnelly, J. McKinley, J.D. Hansen, R. Morgan, D. Pirrie,

558 M. Harrison, The use of geoscience methods for terrestrial forensic searches. *Earth Sci. Rev.*

559 114 (2012a) 108-123. DOI:10.1016/j.earscirev.2012.05.006

560

561 J.K. Pringle, J.R. Jervis, J.D. Hansen, N.J. Cassidy, G.M. Jones, J.P. Cassella, Geophysical

562 monitoring of simulated clandestine graves using electrical and Ground Penetrating Radar

563 methods: 0-3 years, *J. For. Sci.* 57 (2012b) 1467-1486. DOI:10.1111/j.1556-

564 4029.2012.02151.x

565

566 J.K. Pringle, J.R. Jervis, Electrical resistivity survey to search for a recent clandestine burial of

567 a homicide victim, UK, *For. Sci. Int.* 202 (2010) e1-e7. DOI:10.1016/j.forsciint.2010.04.023

568

569 A. Ruffell, A. McCabe, C. Donnelly, B. Sloan, Location and assessment of an historic (150–160
570 years old) mass grave using geographic and ground penetrating radar investigation, NW
571 Ireland, *J. Forensic Sci.* 54 (2009), 382–394. DOI:10.1111/j.1556-4029.2008.00978.x

572

573 A. Ruffell, B. Kulesa, Application of geophysical techniques in identifying illegally buried
574 toxic waste, *Env. For.* 10 (2009) 196–207. DOI: 10.1080/15275920903130230

575

576 E.M.J. Schotmans, J.N. Fletcher, J. Denton, R.C. Janaway, A.S. Wilson, Long-term effects of
577 hydrated lime and quicklime on the decay of human remains using pig cadavers as human
578 body analogues: field experiments. *For. Sci. Int.* (2014) 141.e1-e13.

579 DOI:10.1016/j.forsciint.2013.12.046

580

581 B. Sloane, *The Black Death in London*, The History Press, Stroud, UK, 2011. ISBN: 978-0-
582 7524-2829-1

583

584 P. De Smedt, M. Van Meirvenne, T. Saey, E. Baldwin, C. Gaffney, V. Gaffney, Unveiling the
585 prehistoric landscape at Stonehenge through multi-receiver EMI, *J. Arch. Sci.* 50 (2014) 16-
586 23. DOI:10.1016/j.jas.2014.06.020

587

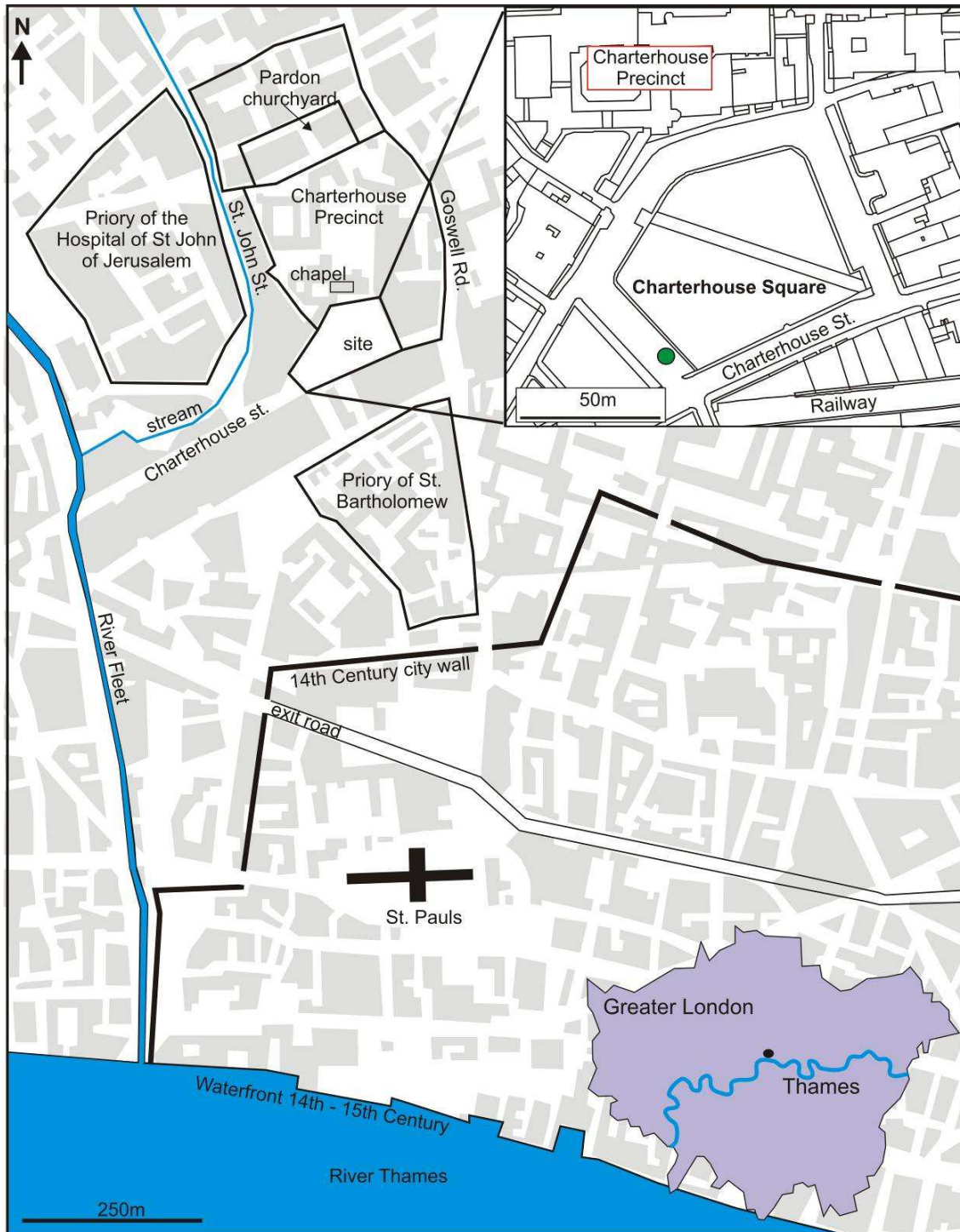
588 P. Temple, P 2010. *The Charterhouse*, Survey of London Monograph 18, Yale University Press

589 for English Heritage, p.30. ISBN: 9780300167221

590

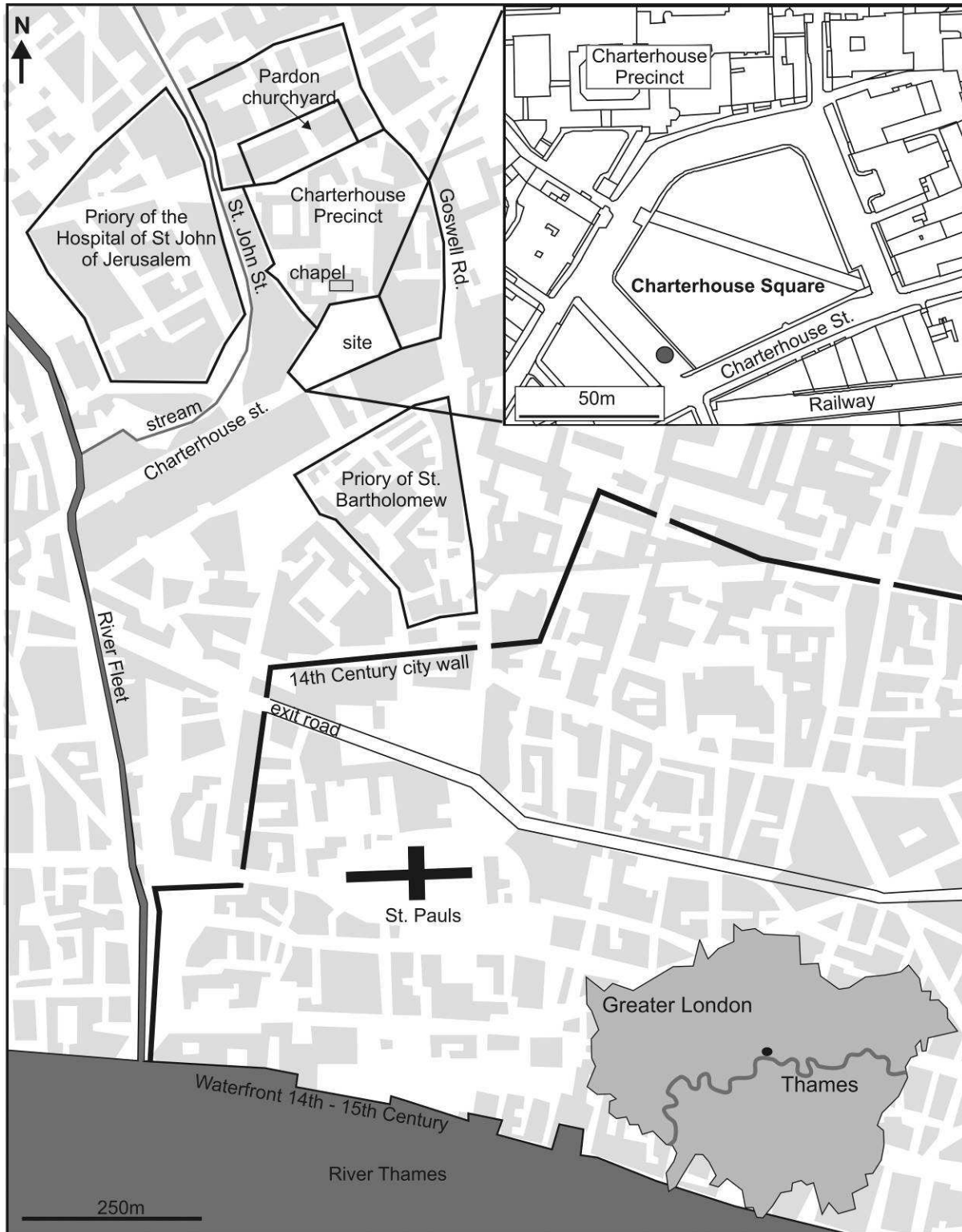
591

ACCEPTED MANUSCRIPT

592 **Figures:**

593

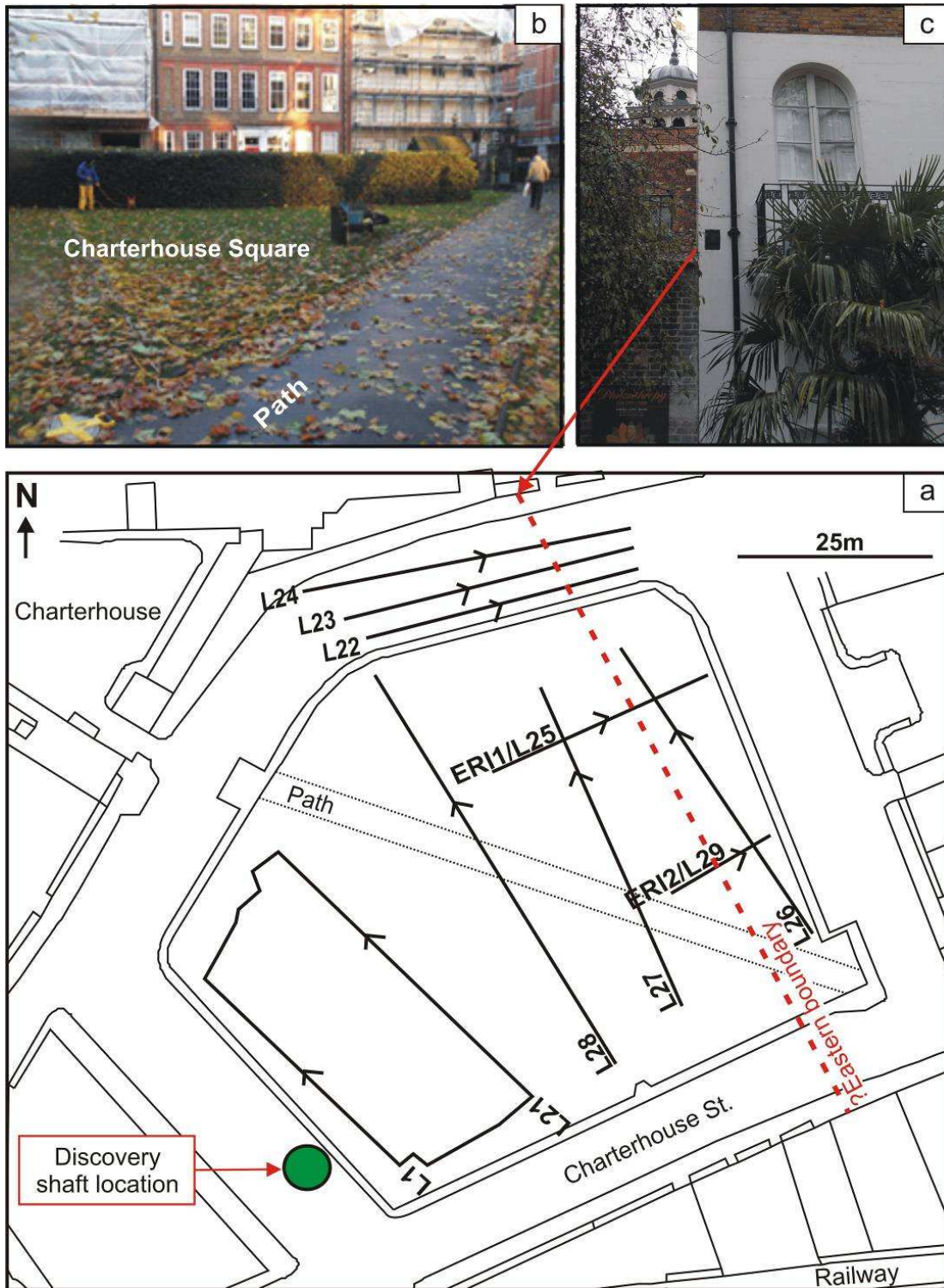
594 **Figure 1:** Map of the general and specific survey area (with location inset) and relevant595 *Medieval features superimposed (after MoLAS, 2013).*



596

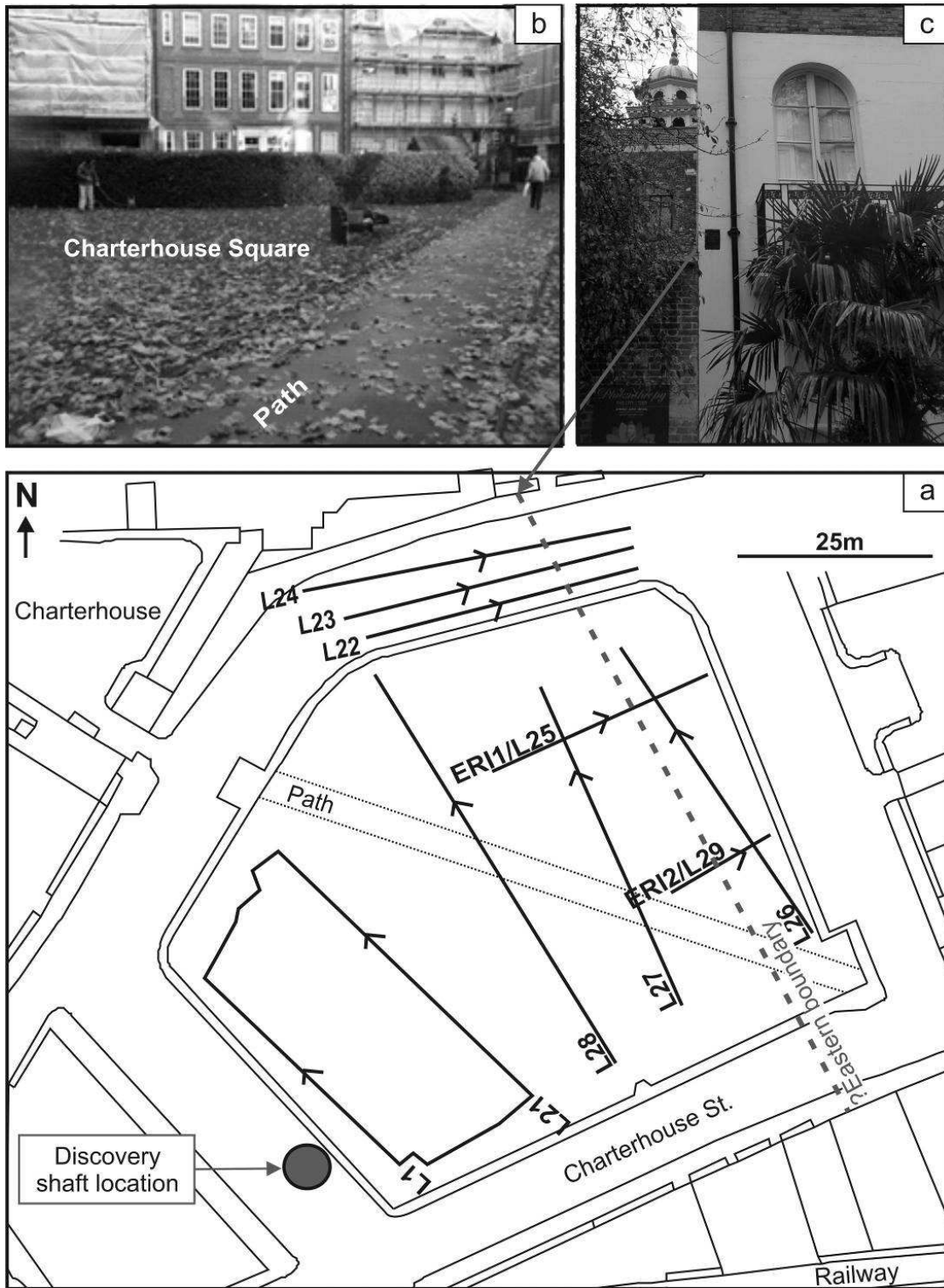
597 **Figure 1:** Map of the general and specific survey area (with location inset) and relevant598 *Medieval features superimposed (after MoLAS, 2013).*

599



600

601 **Figure 2:** a) Mapview of Charterhouse Square showing discovery shaft location (circle),
 602 named geophysical survey lines and orientations, parish boundary (dotted), b) site
 603 photograph and c) parish boundary building plaque.

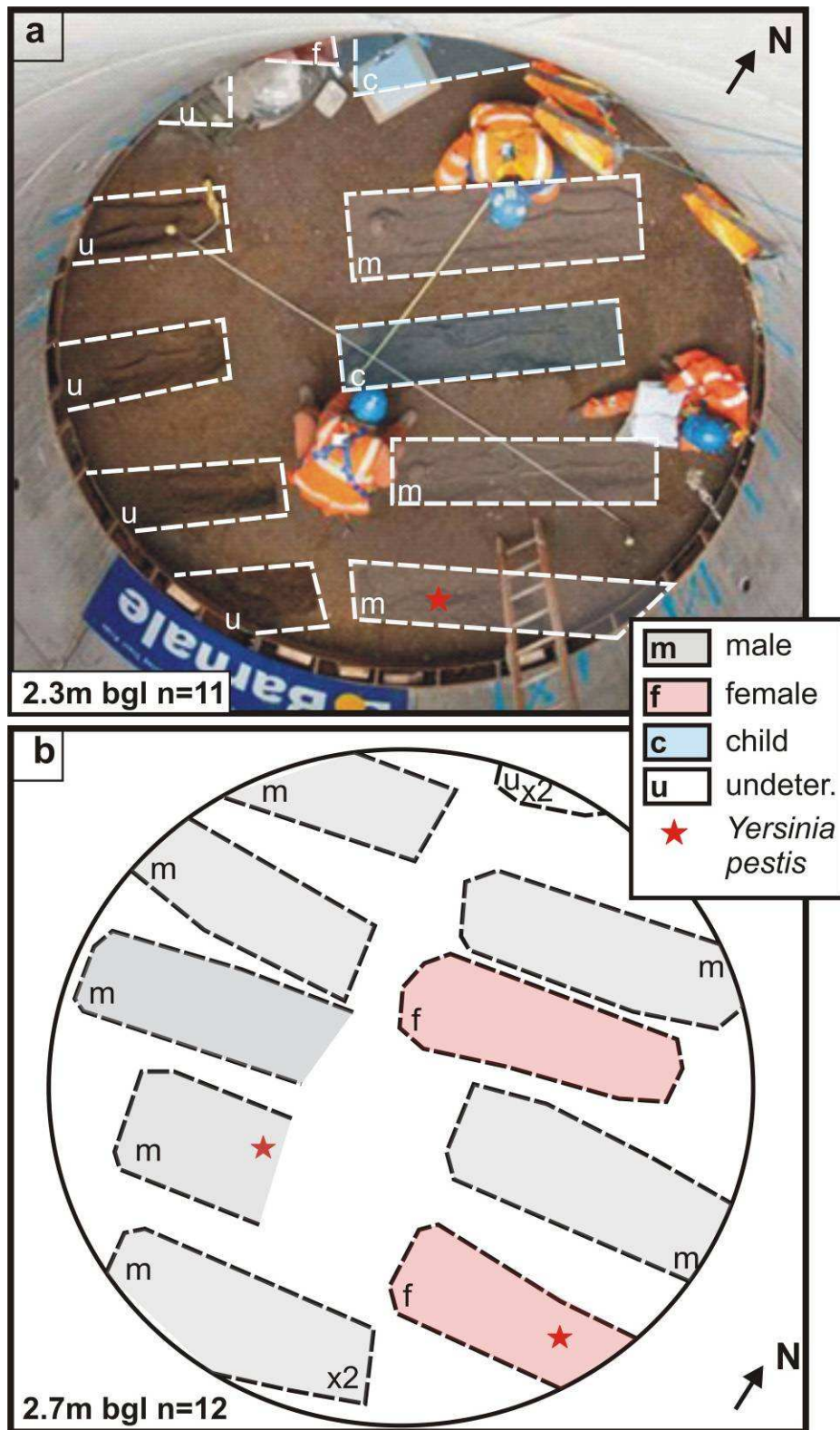


604

605 **Figure 2:** a) Mapview of Charterhouse Square showing discovery shaft location (circle),

606 named geophysical survey lines and orientations, parish boundary (dotted), b) site

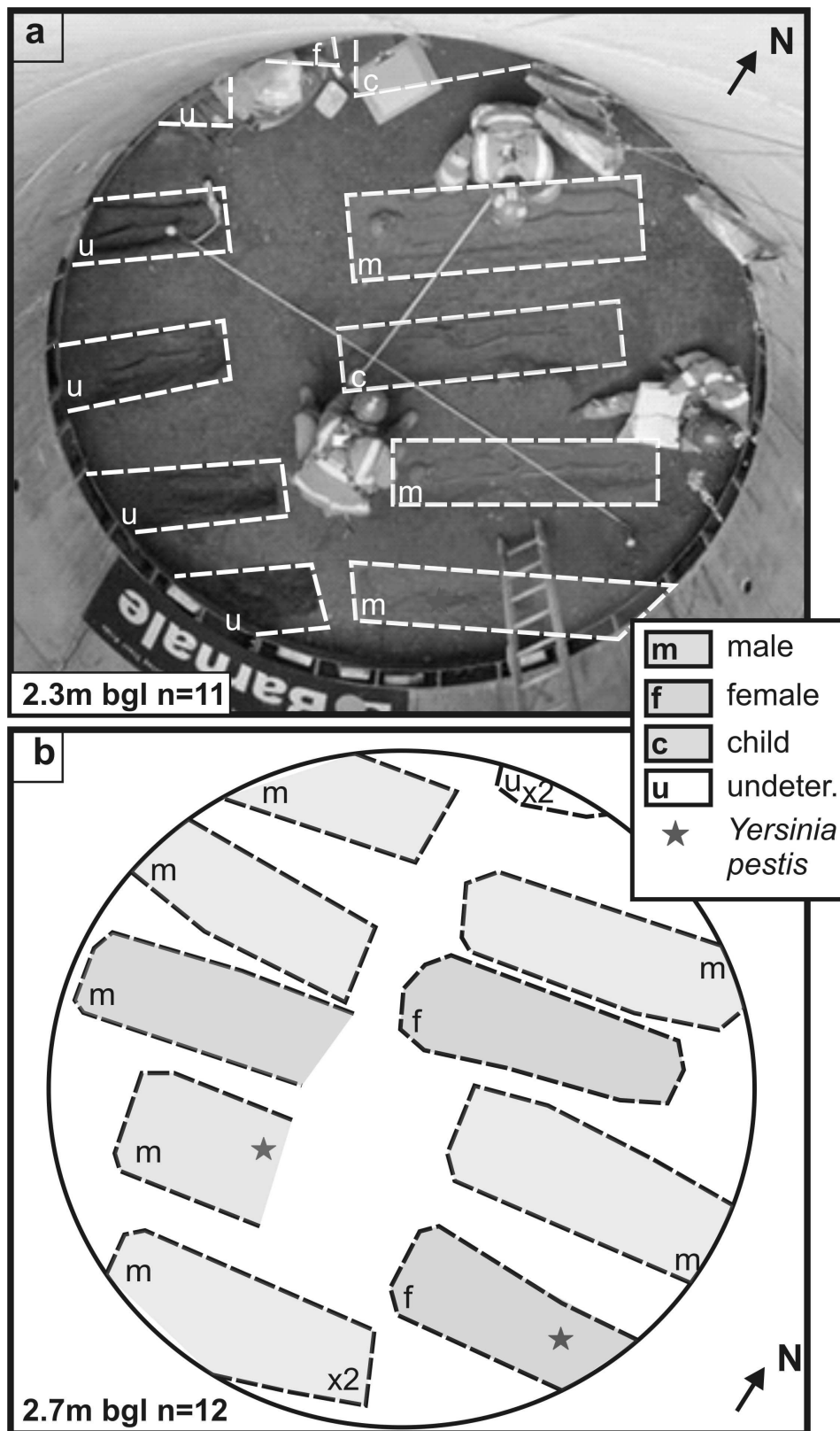
607 photograph and c) parish boundary building plaque.



608

609 **Figure 3:** Mapview of shaft discovered earth-cut graves with identified burials and confirmed610 *Yersinia pestis* (see keys) at (a) 2.3 m and (b) 2.7 m BGL respectively (**Fig. 2** for location).

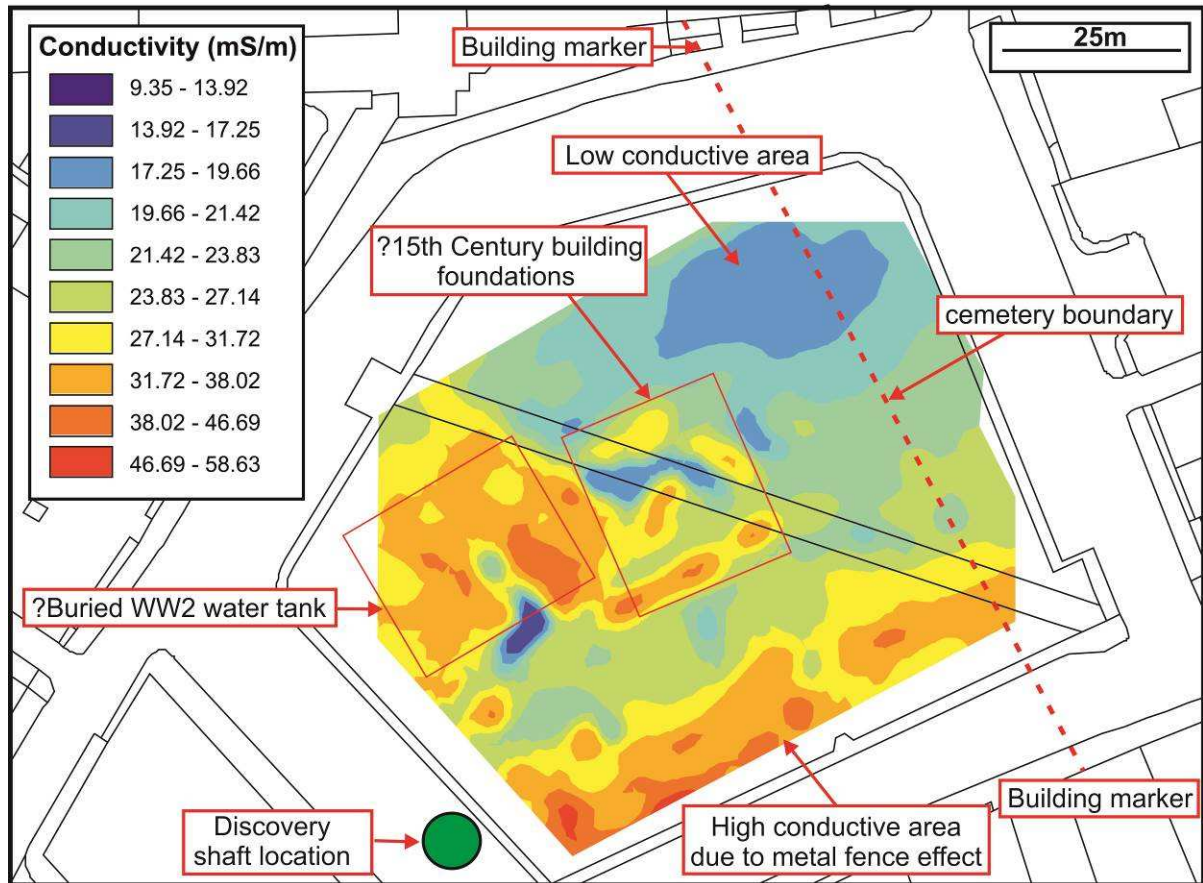
611 Two graves discovered at 2.5 m BGL not shown. Modified from MoLAS (2013).



612

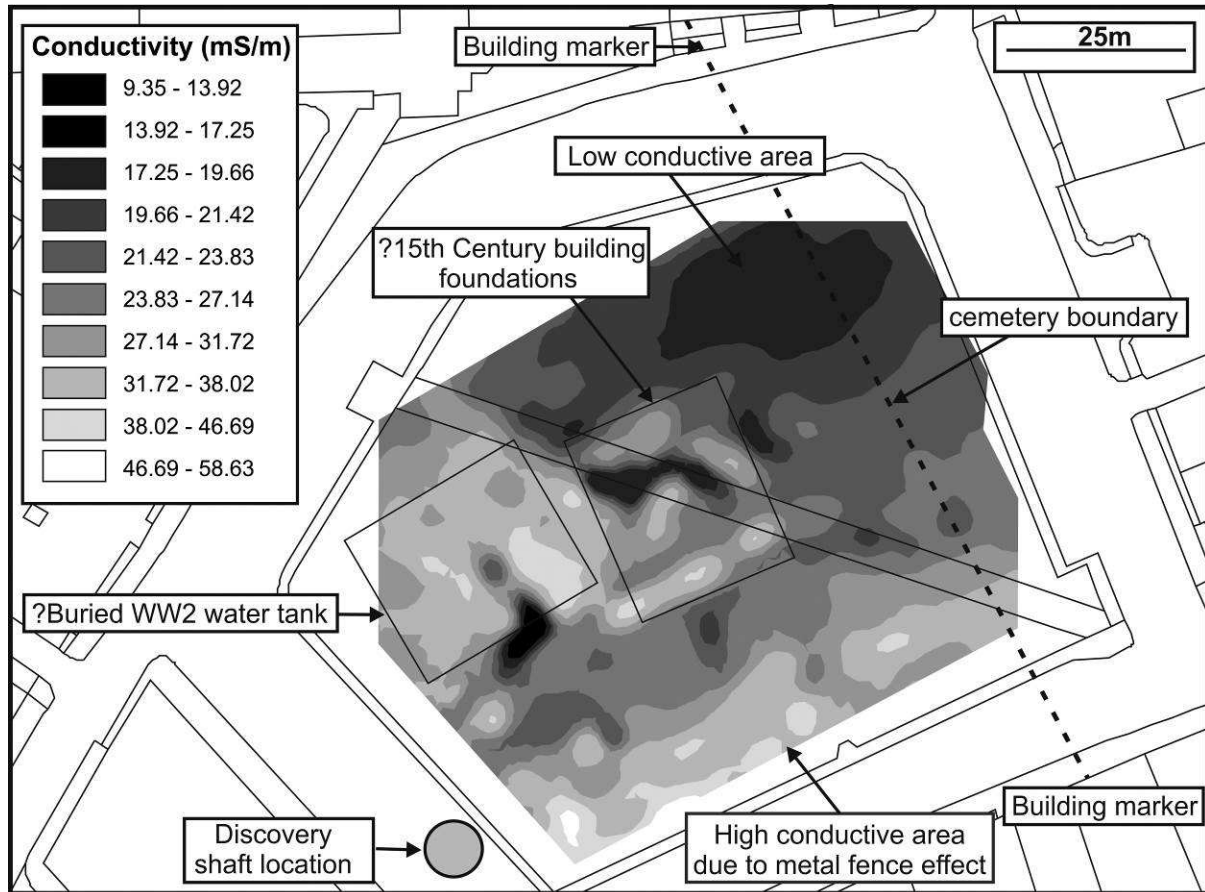
613 **Figure 3:** Mapview of shaft discovered earth-cut graves with identified burials and confirmed614 *Yersinia pestis* (see keys) at (a) 2.3 m and (b) 2.7 m BGL respectively (**Fig. 2** for location).

615 Two graves discovered at 2.5 m BGL not shown. Modified from MoLAS (2013).



616

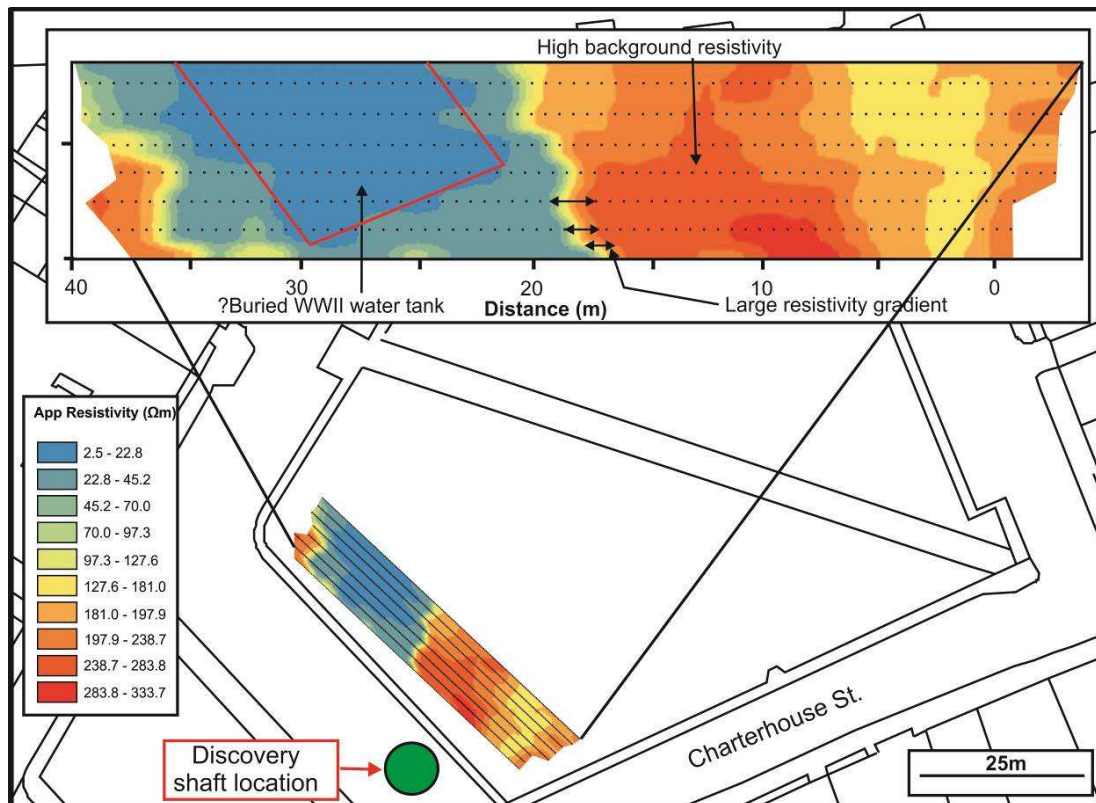
617 **Figure 4:** Processed electro-magnetic (EM) conductivity Quadrature dataset with contoured
 618 digital surface (see key) and annotated interpretations.



619

620 **Figure 4:** Processed electro-magnetic (EM) conductivity Quadrature dataset with contoured
 621 digital surface (see key) and annotated interpretations.

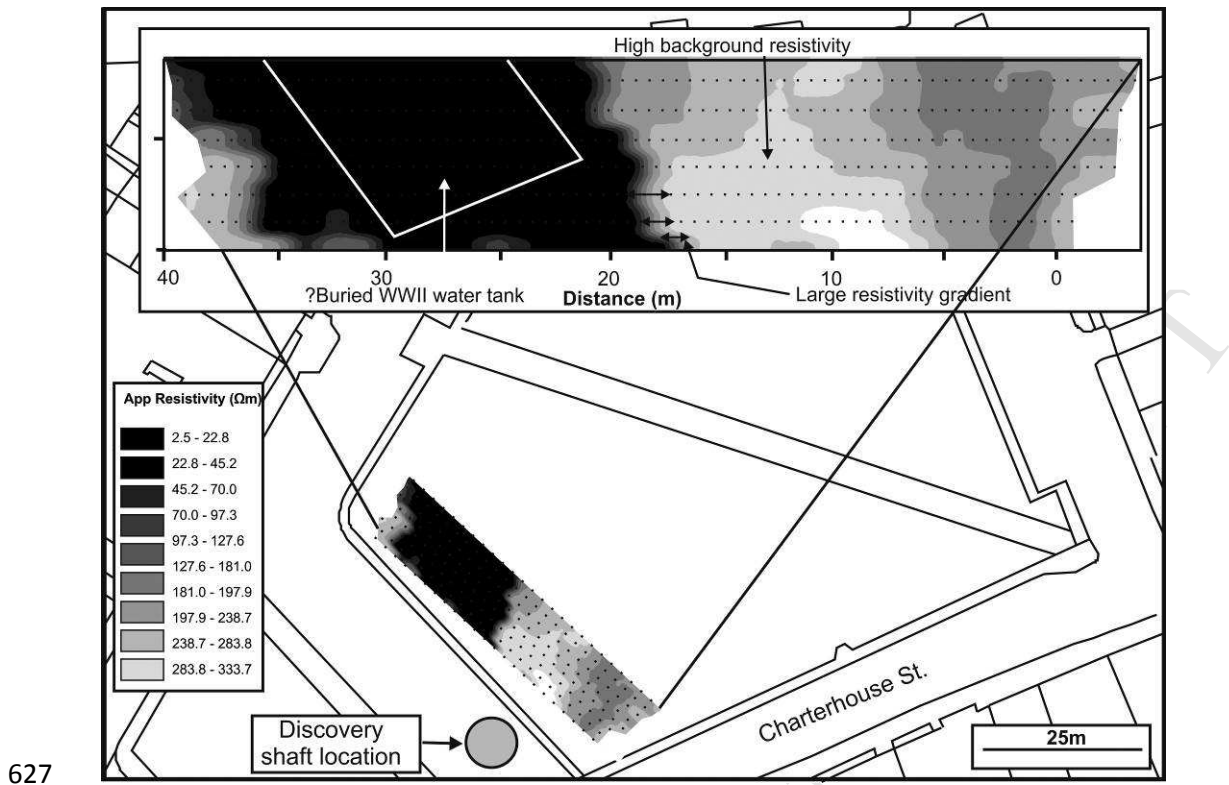
622

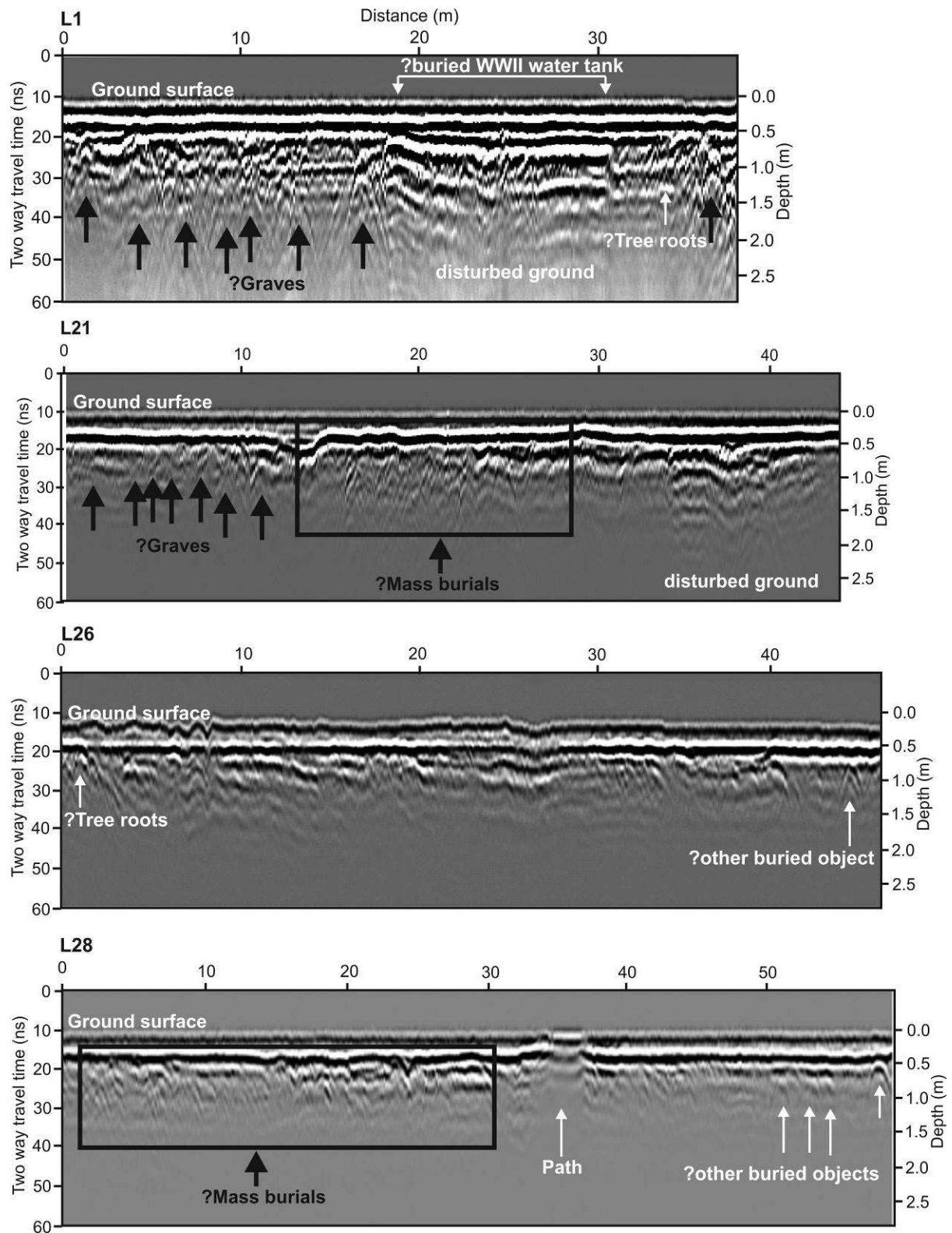


623

624 **Figure 5:** Processed electrical resistivity dataset with contoured digital surface (see key) and
 625 annotated interpretations.

626



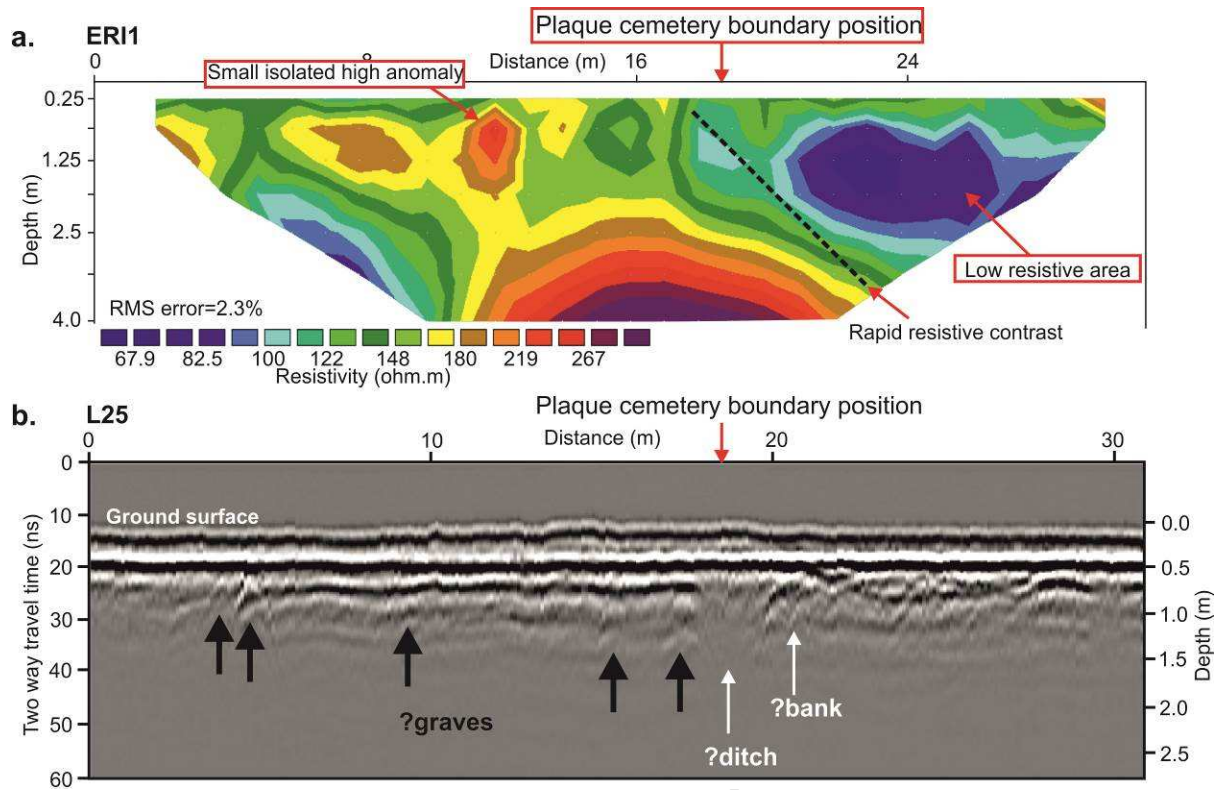


630

631 **Figure 6:** Selected GPR 2D interpreted profiles all orientated south to north(Fig. 2 for

632 location). Note L26 is to the east of the parish boundary.

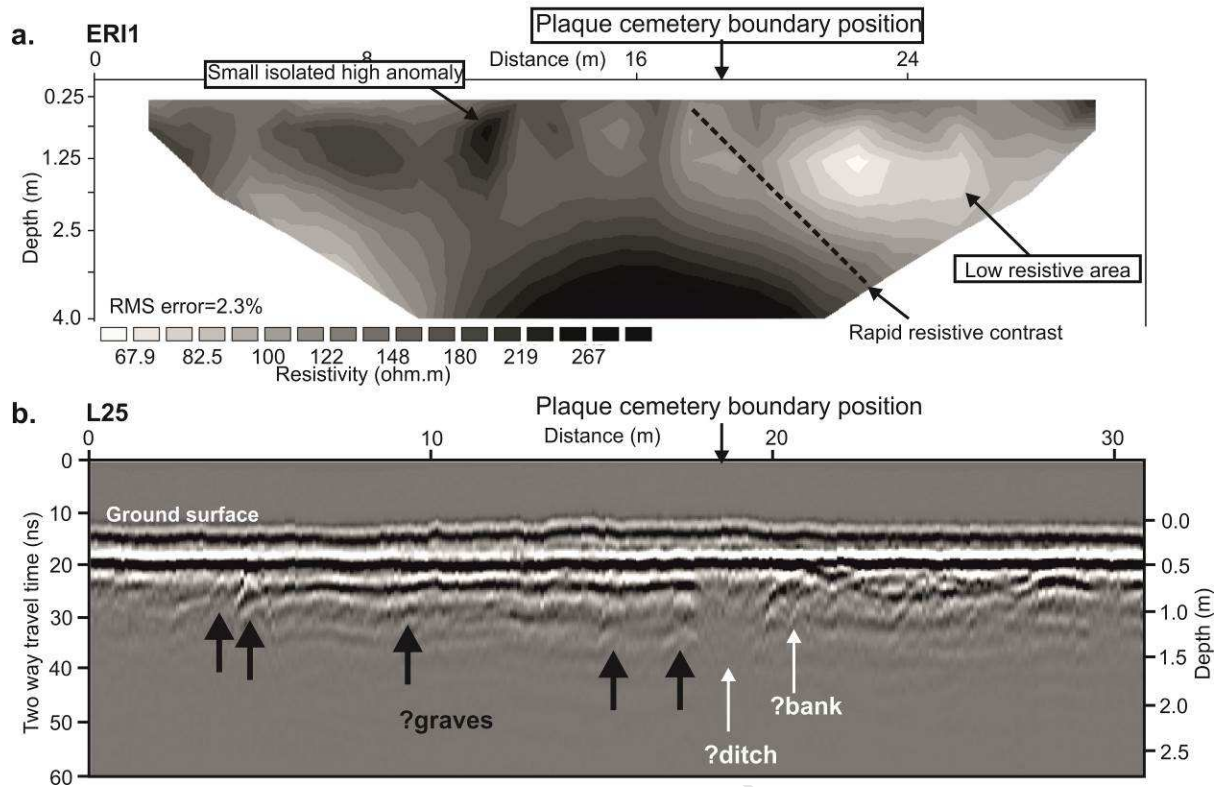
633



634

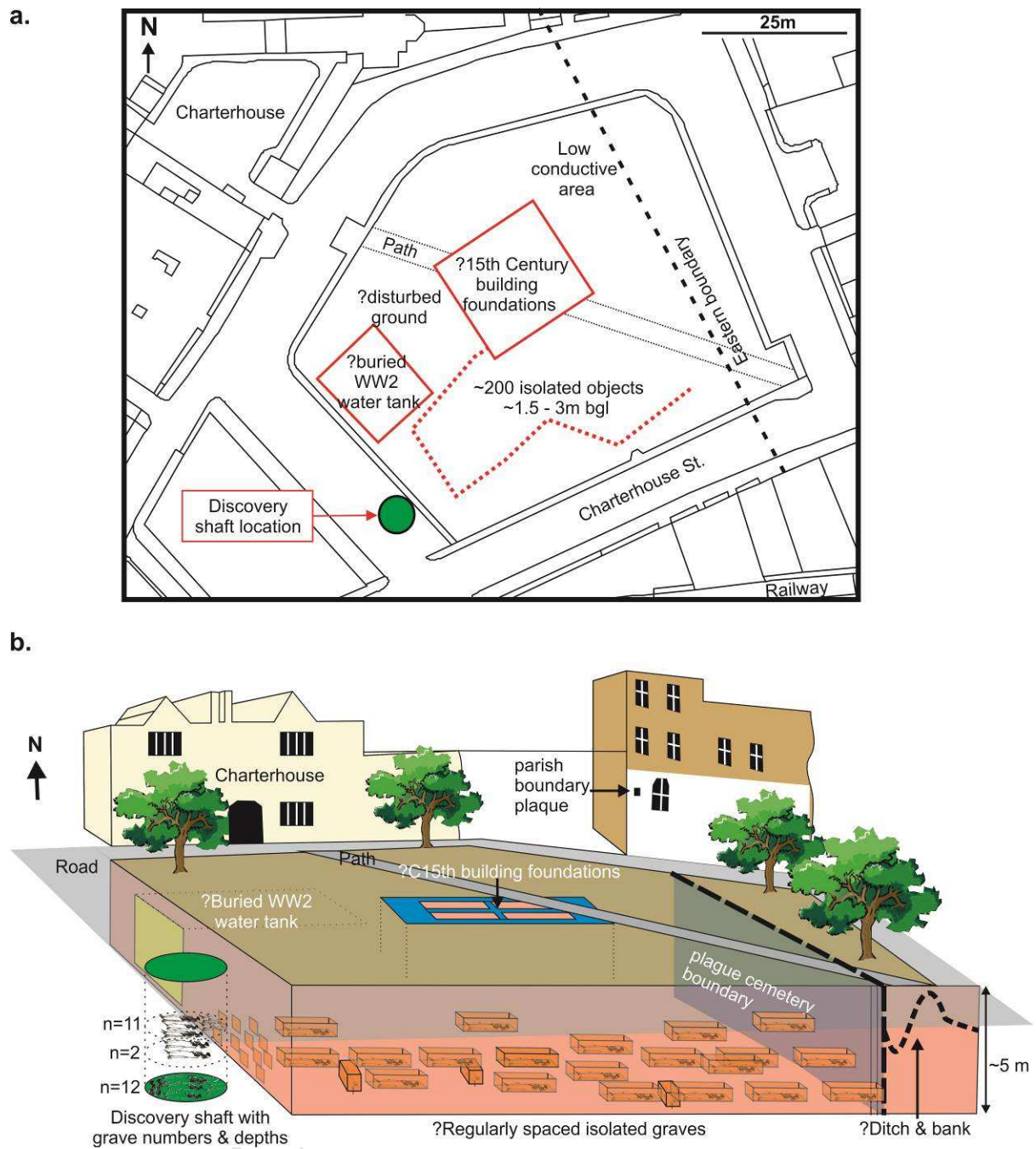
635 **Figure 7:** a) ERI1 and b) 2D GPR interpreted profile orientated west to east across the parish
 636 boundary (**Fig. 2** for location).

637



638

639 **Figure 7:** a) ERI1 and b) 2D GPR interpreted profile orientated west to east across the parish640 boundary (**Fig. 2** for location).



641

642 **Figure 8:** Summary showing geophysical interpretation, A) 2D Planview map and B) 3D

643 schematic visualisation of the site that is not to scale.

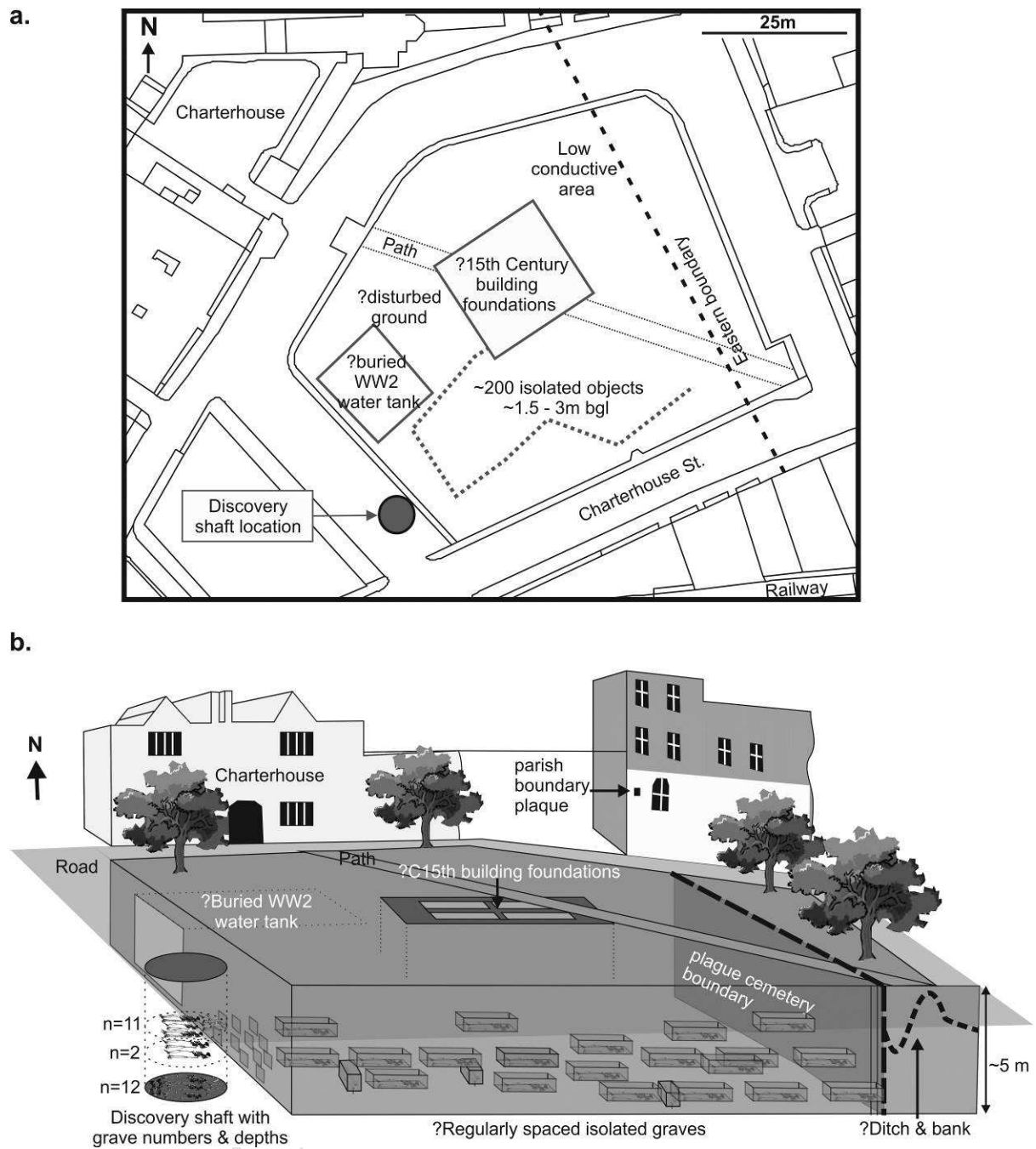


Figure 8: Summary showing geophysical interpretation, A) 2D Planview map and B) 3D schematic that is not to scale.

650

Site targets identified	Documented Records	Geophysical responses
Historic burials	Suggested burials in mass pits	GPR data imaged ~200 burials in SW of square, isolated, evenly spaced and ~1.5 m- 3 m bgl (Fig. 6/8)
Burial ground eastern boundary	Suggested parish boundary and ditch and bank form	2D ERI and GPR profiles (Fig. 7) agreed both boundary position and ditch and bank geometries
Demolished building foundations	Two chapels and meat kitchen recorded onsite	~20 m ² square-shaped EM anomalies in central area (Fig. 4)
WW2 fire-fighting water tanks	Present 1940 but perhaps removed	~15 m ² object in NW of square (Fig. 4), conductive, low resistance & strong horizontal top/base radar reflectors

651

652 **Table 1.** List of targets identified in this study, documented records and their geophysical
653 responses (**Fig. 8** for location).

654

Highlights:

- Multiple skeletons discovered during Europe's largest construction project
- Near-surface geophysical survey of Charterhouse Square revealed hundreds more
- Burials were surprisingly isolated and not in mass burial pits
- Burials were also phased and in different orientations
- Radiocarbon dating and aDNA tooth analysis confirmed Black Death victims
- Study has implications for other mass burial searches

